Environmental Science
Water Research & Technology

ROYAL SOCIETY OF CHEMISTRY

PAPER

View Article Online
View Journal

Cite this: DOI: 10.1039/c9ew00882a

Balancing water quality and flows in combined sewer systems using real-time control†

Sara C. Troutman, Nancy G. Love and Branko Kerkez *

A new generation of smart and connected stormwater and sewer systems is being enabled by emerging wireless technologies and data algorithms. Stormwater and combined sewer systems can be autonomously controlled (gates, valves, pumps) to allocate storage and adapt to changing inputs. As a result, there is an opportunity to begin viewing the collection system as an extension of the water resource recovery facility (WRRF), whereby flows in the collection system are dynamically controlled to benefit downstream treatment. The dynamic control of collection system storage will allow peak flows to be minimized and solid loads to the plant to be tuned in response to real-time WRRF states as they relate to treatment operation and performance. To that end, this paper presents a formulation of a real-time load-balancing algorithm to control distributed storage assets in the collection system, with objectives of improving flow and water quality dynamics at inflow to a treatment plant. We illustrate that this load-balancing approach can successfully attenuate wet-weather peaks and minimize dry-weather oscillations. The parameterization of the control algorithm is assessed in the context of competing objectives at the downstream WRRF and broader collection system (*e.g.* sediment loads, peak flows, flooding, and solids accumulation in the sewer system). By applying this control algorithm and analysis to an established case study, we identify a range of parameter values that provide most desirable performance across a number of system-wide objectives. Specifically, we discover a band of desirable performance, which not only improves inflow into the WRRF, but simultaneously reduces flooding and sedimentation in the collection system.

Received 2nd October 2019,
Accepted 5th February 2020

DOI: 10.1039/c9ew00882a

rsc.li/es-water

Water impact

New technologies create the opportunity to control the sewer system as an extension of the treatment plant. By dynamically controlling water in existing collection system infrastructure, flow management and treatment can benefit system performance while reducing potential adverse impacts (flooding, sediment accumulation) across the system. We present an open-source control algorithm for combined sewers and show how benefits at the treatment plant do not always have to come with major drawbacks for the operation of the collection system.

1 Introduction

New technologies and data algorithms show promise of enabling a new generation of smart and connected stormwater and sewer systems. These systems process distributed sensor data to predict flows, levels, and other relevant states to control valves, gates, and pumps. This enables entire collection systems to be adapted to changing storms and inputs in real-time, promising to reduce flooding and improve water quality by making more effective use and achieving high performance out of existing infrastructure. Most studies evaluating real-time control technologies have focused on water quantity objectives, in particular the reduction of overflows and flooding. Comparatively little emphasis has been placed on the role of smart stormwater systems in controlling water quality. While not regulated explicitly, controlling water quality within the collection system stands to reduce effluent loads at WRRFs by improving treatment operations, which should ultimately lead to improved water quality in receiving waters.

In the case of combined sewer systems, the same pipes are used to convey stormwater and wastewater. Water resource recovery facilities (WRRFs), also known as wastewater treatment plants (WWTPs), receive these combined flows. This challenges treatment efficiency due to fluctuations in flows and pollutant loads during storm events. Given the advent of smart stormwater systems, there is an opportunity to begin viewing the collection system as a tool for assisting the treatment plant by providing desirable

University of Michigan, Civil and Environmental Engineering, Ann Arbor, MI, USA. E-mail: bkerkez@umich.edu

† Electronic supplementary information (ESI) available. See DOI: 10.1039/c9ew00882a

inflows. By dynamically controlling flows in these combined sewer systems, peak flows to the plant can be minimized, while solids loads to the plant, for example, can be controlled in response to real-time WRRF states, such as nutrient loading or treatment capacity. In this paper, we evaluate the potential benefits of such an approach by investigating how the collection system can be controlled methodically in a real-time and coordinated approach to shape inflows and loads going to a receiving WRRF.

The specific contributions of this paper are:

- The formulation of a real-time load-balancing algorithm to control distributed storage assets in the collection system, to improve wet-weather flows and water quality at a receiving point, and
- An evaluation of this algorithm under simulated conditions, with an analysis of trade-offs arising during the balancing of flows and total suspended solids (TSS) going to a WRRF.

We also provide a fully open-sourced implementation of the algorithm, with all code, model of the study, and results shared to promote transparency, reproducibility, and broader adoption.

1.1 Background

1.1.1 Water quality and combined sewer systems. Combined sewers integrate stormwater and wastewater flows into the same pipe network, which is connected to the downstream WRRF. Thus, the WRRF often experiences abrupt wet-weather impulses on top of more regular dry-weather wastewater inflows. WRRF treatment processes are sensitive to sudden changes in influent dynamics, as these can adversely affect treatment efficacy.[1] For instance, peak flows received at WRRFs can cause washout of settled solids and microorganisms present in preliminary, primary, and secondary treatment units.[2] Beyond wet-weather dynamics, variations in pollutant loads (mass of pollutant per time) received by the WRRF can be driven by seasonal and diurnal wastewater generation patterns, and other factors,[1] further challenging efficiency of WRRF treatment processes.[2,3] One of the most notable and variable pollutant loads includes particulates, such as total suspended solids (TSS). Highly variable TSS inflows can drastically affect treatment performance, either due to lack of treatment capacity or the time required to adjust to inflow variability.[2] It is not surprising, as such, that many research efforts have been dedicated to investigating WRRF resiliency under highly variable loads.[4]

An ideal WRRF influent is one of constant flow and pollutant loads.[5] However, this is not trivial to achieve in the real world, even with the construction of a large equalization basin at the inlet of the WRRF,[6] particularly with large and/or flashy storm events. These large storage structures receive inflow and pump it out at regulated rates so as to not overwhelm the WRRF.[1,3,7] Equalization basins often require extensive footprints (not to mention capital investments), which does not make them a viable option for many communities. In lieu of the construction of expensive storage assets at the inlet of the WRRF, we contend that there is an opportunity to look further upstream, by evaluating the feasibility of using storage capacity that already exists in the sewer network as a means of equalizing inflows to the WRRF. As already demonstrated, control of the collection system can be achieved by controlling already existing assets, such as storage basins, in-line storage dams, gates, valves, and pump stations.[8–12]

Control of the collection system for broader water quality benefits, especially at the WRRF, poses a number of new challenges. It is critical to examine not only the potential of creating close-to-steady-state influent conditions (similar to an equalization basin),[2] but also to evaluate the impacts that these control actions have on the conveyance and performance of the combined sewer system itself. For instance, the control of upstream combined sewer storage to achieve downstream objectives should not place the storage assets at greater risk of overflowing and local flooding. Further, the storage of combined sewer flows within sewer assets could promote the settling of solids across the collection system,[2,13] a challenge for which many upstream assets are often not prepared. In particular, upstream assets are not traditionally designed to accumulate solids, which can require significant effort to resuspend, flush, or remove, and often have no on-site mechanism for solids removal, handling, or treatment. As such, any local benefits of real-time control must consider the system in which it is being deployed and weigh against potential drawbacks, which is a core motivation of this paper.

1.1.2 Benefits of real-time control. Given the recent ubiquity of sensors and connected technologies, the real-time control of urban stormwater systems has witnessed a surge in studies and adoption.[14,15] The idea of autonomously controlled stormwater systems is not necessarily very recent itself; indeed, real-time control for sewer systems has been investigated for some time.[11,16–19] Many of these important studies have laid the groundwork for today's ideas — especially for the control of flooding and overflows — and it is arguably the emergence of readily-available and cost-effective technologies that is fueling efforts to deploy and study smart stormwater systems. Presently, a number of operational systems and test beds exist, including model predictive control (MPC) implementations in Spain[20–22] and Denmark,[23] as well as notable market-based approaches in the USA.[24] The control of separated stormwater systems has also been evaluated, including the deployment of new open-source technologies that can be used to retrofit existing stormwater sites with internet-connected valves.[25,26] These and other studies highlight the potential of real-time control to reduce flooding and overflows. However, much more research is needed to close knowledge gaps underpinning scalable and reliable control algorithms.

Despite progress on real-time flow-based monitoring and control, only a few studies have investigated the benefits of real-time control on water quality. Studies of individual stormwater

basins have shown that TSS can be captured in retention basins by strategically controlling retention time using a valve.[27–29] Similar results have been obtained for dissolved pollutants[30] and bacteria.[31] While highly promising, existing studies have focused on site-scale benefits and were not carried out in the scope of system-scale analysis, which leaves much to be discovered with real-time water quality control of entire systems. As a first step toward a bigger goal, we address this knowledge gap in this paper by formulating a control methodology that coordinates an entire network of storage assets to achieve desired downstream TSS objectives.

1.1.3 Existing control methodologies. A number of system-level control methodologies have risen to prominence for the real-time control of stormwater systems. One of the most studied involves MPC, a mathematical approach grounded in dynamical systems theory.[10,32–37] MPC approximates the flows in a collection system using linearized dynamical equations, which often take the form of mass-balance reservoirs. It has shown great potential to reduce overflows and flooding in combined sewer systems.[33,34,36,37] However, given that the approach assumes linear dynamics both for flows and water quality — which is a considerable simplification of nonlinear water quality dynamics — this approach has been applied to the control of water quality in a limited capacity.[33] Further, there has still been little focus on the influence of weighting between water quantity and quality objectives.

An alternative to MPC is provided in the form of market-based control methods.[24] These approaches treat storage assets in a system (*e.g.*, basins, pipes) as buyers and sellers of a commodity (*e.g.*, pipe or storage capacity). In these formulations, agents trade the commodity as part of a market, where the most stressed assets are allowed to release water *via* "purchases" of capacity. An appealing aspect of this approach is its lack of reliance on explicit system dynamics for the determination of control actions. Rather it only requires measurements of system states (*e.g.*, water level, flow, pollutant concentration). While this does not allow it to be analytically studied like MPC, it does allow for easier implementation and decentralized application. A market-based approach can be viewed as an extension of the "Equal Filling Degree" approach,[38–42] which seeks to balance the filling degree, defined as the actual stored volume relative to the maximum storage volume in a storage structure, among all storage assets in a collection system. This is done at each time step by triggering control actions that increase (or decrease) the stored volume in a particular asset if it is below (or above) the average filling degree among all assets. Borsányi *et al.*[38] extended and compared equal filling to include a downstream structure with a capacity related to the WRRF. The control of all other structures was inversely related to the filling degree of this downstream asset. For example, if the filling degree of this downstream asset increases, the upstream assets decrease their releases to the downstream. Other approaches, such as dynamical systems, neural network-based, and reinforcement learning-based controls have also been proposed as intermediate complexity alternatives to MPC and market approaches, showing good potential to remedy flooding and overflows.[43–45]

Given the general emphasis of these methods on controlling flows and flooding, it is unclear — regardless of actual control methodology — what water quality benefits can be achieved with them when applied with real-time control at the scale of the collection system. Integrating water quality optimization into existing real-time flow control approaches requires significant computational overhead, especially when considering the need to formulate, linearize, and analyze dynamics with approaches such as MPC. We contend that before exploring more complex control implementations, a more general analysis of the trade-offs and benefits of controlling system-level water quality is warranted. To that end, we introduce a control technique — coined load balancing — of relatively low complexity but of high flexibility to simulate a broad range of conditions focused on controlling drainage systems for water quality. We formulate the technique in a model-free context that allows us to specify flow and water quality objectives by tuning a small number of intuitive parameters. By evaluating the range of trade-offs that exist when both water flows and water quality are controlled, this study provides an assessment of real-time control benefits that can be expanded in the future using more complex control formulations.

2 Methods

We present a load balancing control methodology built around a set of core parameters, the analysis of which will provide insight into upstream and downstream trade-offs when controlling a system in real-time. The control algorithm is evaluated on an established case study,[46] based on a real world-inspired combined sewer system.

2.1 Load balancing control algorithm

Consider a collection system with n total network storage assets (*e.g.*, tanks, in-line storage facilities) distributed into a set of controllable assets, I_C, and a set of uncontrollable assets I_U. At time step t, each asset i is described by a vector of states of interest

$$S_i(t) = \begin{bmatrix} S_i^1(t) \\ \vdots \\ S_i^d(t) \end{bmatrix},$$

where the d elements of the vector include relevant states that describe the asset (*e.g.* water level, outflows, TSS concentration). Each asset also has a corresponding setpoint vector $S_i^*(t)$ which describes the desired states of the asset (*e.g.* overflow conditions, maximum desired flows, desired loads). The state vector for each asset is user-specified and includes those states that are most relevant to any given application. In simple applications, one may only seek to control water levels (*e.g.* flooding), but in more complex

scenarios one can expand the state vectors to include water quality or other factors.

Some assets may be considered more critical in the system than others. For example, operators may want to release water sooner or avoid overflows at one location more than others due to specific preferences or regulations. To capture this user preference, we introduce the system importance factor α_i for each asset and state

$$\alpha_i = \begin{bmatrix} \alpha_i^1 \\ \vdots \\ \alpha_i^d \end{bmatrix}.$$

This captures a relative weight of one asset's state over another in the system — with a higher number reflecting relatively larger importance in the system. For controllable assets ($i \in I_C$), the importance of each asset is also extended to include an instantaneous component. For example, a storage tank that is close to capacity or overflowing should be considered briefly more important than those that are not full, so as to minimize overflows or flooding. To capture this notion, we introduce an instantaneous, or short-term, importance for each asset and state

$$\gamma_i(t) = \begin{bmatrix} \gamma_i^1(t) \\ \vdots \\ \gamma_i^d(t) \end{bmatrix}, \qquad \gamma_i^1(t) = \frac{e^{\rho S_i^1(t)} - 1}{e^{\rho} - 1}.$$

This exponential factor is computed element-wise for each time step and state within the state vector S_i and can be tuned to reflect user preferences. Given the state of the asset, the instantaneous importance weight ρ can be tuned to reflect how stressed an asset is at any given point in time. By analogy, ρ could encapsulate the comfort level of an operator (*e.g.*, release proportional to water level *vs.* prioritize an asset only if it is close to full). For example, if storage capacity is used as an indicator of importance, with $\rho = 1$ the instantaneous importance of the asset increases nearly linearly with water level (Fig. 1). With $\rho = 100$ the asset would be considered important only if it is close to capacity. If asset i is uncontrollable ($i \in I_U$), its importance is not discounted in this state-dependent manner because, regardless of state, uncontrollable assets will passively release flows (thus $\gamma_i = 1$). Finally, the overall importance $\beta_i(t)$ is calculated by simply multiplying the system importance with the instantaneous importance of each asset:

$$\beta_i(t) = \alpha_i \odot \gamma_i(t),$$

where $\odot$ indicates the Hadamard, or entrywise, product between α_i and $\gamma_i(t)$ (that is $\beta_i^1(t) = \alpha_i^1 \gamma_i^1(t)$, *etc.*). At any point in time, this overall importance factor is used to determine how much water is released from each controllable asset. This is accomplished by computing the importance-weighted average, which compares the state of each asset to its desired setpoint

$$\bar{C}(t) = \frac{1}{n} \sum_{i=1}^{n} \beta_i(t)^{\top} \left(S_i(t) - S_i^*(t) \right).$$

Note that this $\bar{C}$, the importance-weighted average, includes all n assets, both controllable and uncontrollable. At each time step t, the set of controllable assets that will release water, $J \subseteq I_C$, is determined as those whose importance-weighted deviation is greater than the average; that is,

$$J = \left\{ j : \beta_j(t) \cdot \left(S_j(t) - S_j^*(t) \right) > \bar{C}(t) \right\}.$$

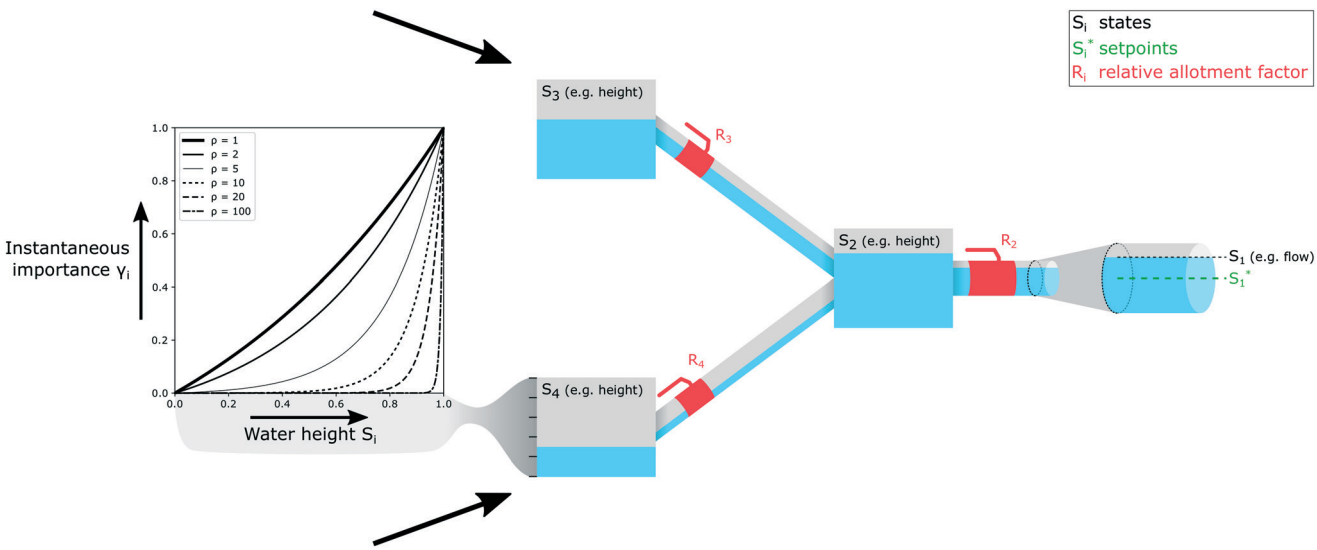

Fig. 1 Graphical representation of control procedure. Valves are controlled to release water from controlled assets, relative to an allotment factor that is assigned to each controlled asset. The instantaneous importance weight ρ can be tuned to determine when water is released from each asset.

Assets below this average (*e.g.*, storage tanks with available capacity) do not release flows. Furthermore, the amount of water released from each of these assets in set J is computed as a relative allotment factor $R_j(t)$ for asset j. This relative allotment factor is defined as the importance-weighted deviation normalized within set J; that is,

$$R_j(t) = \frac{\beta_j(t)^\top \left(S_j(t) - \mathbf{S}_j^*(t)\right) - \overline{C}(t)}{\sum_{k\in J}\left(\beta_k(t)^\top \left(S_k(t) - \mathbf{S}_k^*(t)\right) - \overline{C}(t)\right)},$$

where $\sum_{k\in J}$ is the summation of the importance-weighted deviation over all assets that will release water (*i.e.*, each asset k in set J). This allotment factor R_j simply assigns the fraction of a downstream asset's capacity that will be allotted to an upstream asset j and is then multiplied by available downstream capacity to determine how much to release from each upstream storage asset.

This procedure is summarized in Algorithm 1

Algorithm 1: Load balancing control

Inputs: S_i (states), S_i^* (setpoints), α_i (system importances), ρ (instantaneous importance weight), I_C (controllable assets), I_U (uncontrollable assets)

for $t \in T$ **do**
  for $i \in (I_C \cup I_U)$ **do**
    if $i \in I_C$ **then**
      $\gamma_i(t) \leftarrow \frac{e^{\rho S_i(t)} - 1}{e^{\rho} - 1}$
    else
      $\gamma_i(t) \leftarrow 1$
    $\beta_i(t) \leftarrow \alpha_i \odot \gamma_i(t)$
    $\overline{C}(t) \leftarrow \frac{1}{n}\sum_{i=1}^{n} \beta_i(t)^\top \left(S_i(t) - \mathbf{S}_i^*(t)\right)$
    if $i \in I_C$ **and** $\beta_i(t)^\top \left(S_i(t) - \mathbf{S}_i^*(t)\right) > \overline{C}(t)$ **then**
      $J \leftarrow J \cup \{i\}$
  for $j \in J$ **do**
    $R_j(t) \leftarrow \frac{\beta_j(t)^\top \left(S_j(t) - \mathbf{S}_j^*(t)\right) - \overline{C}(t)}{\sum_{k\in J}\left(\beta_k(t)^\top \left(S_k(t) - \mathbf{S}_k^*(t)\right) - \overline{C}(t)\right)}$

2.2 Case study

2.2.1 Scenario and implementation. All code for implementation of the above algorithm is provided open-source in a public web repository (https://github.com/stroutm/LBCsewer). The algorithm is applied to Scenario epsilon of the Open-Storm.org pystorms Python package (open-storm.org/pystorms).[46] This package uses PySWMM,[47] a Python wrapper for the popular U.S. Environmental Protection Agency Stormwater Management Model (SWMM), to run and dynamically control a sewer model throughout a simulation. In PySWMM's step-by-step execution, specified states (*e.g.*, depths, inflows, pollutant concentrations) are collected, calculations for control actions can be performed in Python, and control asset settings (*e.g.*, gate positions) are set before the next simulation step is run.

The case study used for this paper is Scenario epsilon of the pystorms package.[46] It represents a combined sewer network with a subcatchment area of 67 km^2 (26 mi^2) and eleven in-line storage assets with controllable orifices (Fig. 2). This scenario was selected due to network topology (*i.e.*, storage assets in series and parallel) and multiple objectives: regulation of flow and TSS load at the network outlet (WRRF inlet) and the need to reduce flooding at each of the upstream storage assets. The collection system receives rainfall runoff, as well as steady, dry-weather inputs to reflect wastewater diurnal patterns (Fig. S1†). More information regarding this network can be found in the pystorms package documentation (open-storm.org/pystorms).[46]

There is one downstream WRRF (node 1 in the network) (I_U = {1}), which receives flows from the entire upstream network. Applying the control procedure described above, for this WRRF we are interested in flow (q) and TSS load (tss) inflow states:

$$S_1(t) = \begin{bmatrix} S_1^{q}(t) \\ S_1^{tss}(t) \end{bmatrix}, \qquad S_1^*(t) = \begin{bmatrix} S_1^{q*}(t) \\ S_1^{tss*}(t) \end{bmatrix}, \qquad \alpha_1 = \begin{bmatrix} \alpha_1^{q} \\ \alpha_1^{tss} \end{bmatrix}.$$

The flow and TSS load states are normalized to the dry-weather flows in the system. The goal is to maintain all controlled inflows (volume per time) or loads (pollutant mass per time) (both wet and dry) at the WRRF below the average dry-weather flow. This is an aggressive strategy that may not be realizable, but it presents an upper bound on performance. Striving for dry-weather inflows during wet-weather conditions should results in benefits compared to the baseline.

The collection system also contains eleven controllable in-line storage assets (I_C = {2, …, 12}). Each storage asset is a conveyance pipe, whose outlet is controlled through a valve or inflatable dam. When closed, the water level in the pipe rises and the available in-line storage capacity is used to keep flow from going downstream. The state for each of these assets is the water level (h), which is normalized to the maximum water depth in each controlled pipe. The setpoint for these assets is set to zero

$$S_i(t) = \left[S_i^h(t)\right], \qquad \mathbf{S}_i^*(t) = \left[S_i^{h*}(t)\right] = [0]$$

to reflect the desire to empty the pipes and not keep water in the system, if possible. The case study considers each of these in-line storage assets as equally important within the system (the system importance for each asset $i \in I_C$ is $\alpha_i = 1$).

The load balancing control algorithm provides the proportion of downstream capacity to be allocated to each controllable upstream storage asset j *via* the relative allotment factor R_j. To translate this factor into control decisions (*e.g.*, gate positions), the flow to be released from each upstream asset is determined as a balance between the downstream objective setpoints, S_1^{q*} and S_1^{tss*}, weighted by the system importance values, α_1^{q} and α_1^{tss}. In this study, since α_1^{q} and α_1^{tss} are the weights assigned to the downstream states, larger values of α_1^{q} and α_1^{tss} indicate higher importance for these downstream objectives relative to upstream. Note that for implementation with water quality-based control, measurements representative of average TSS concentrations

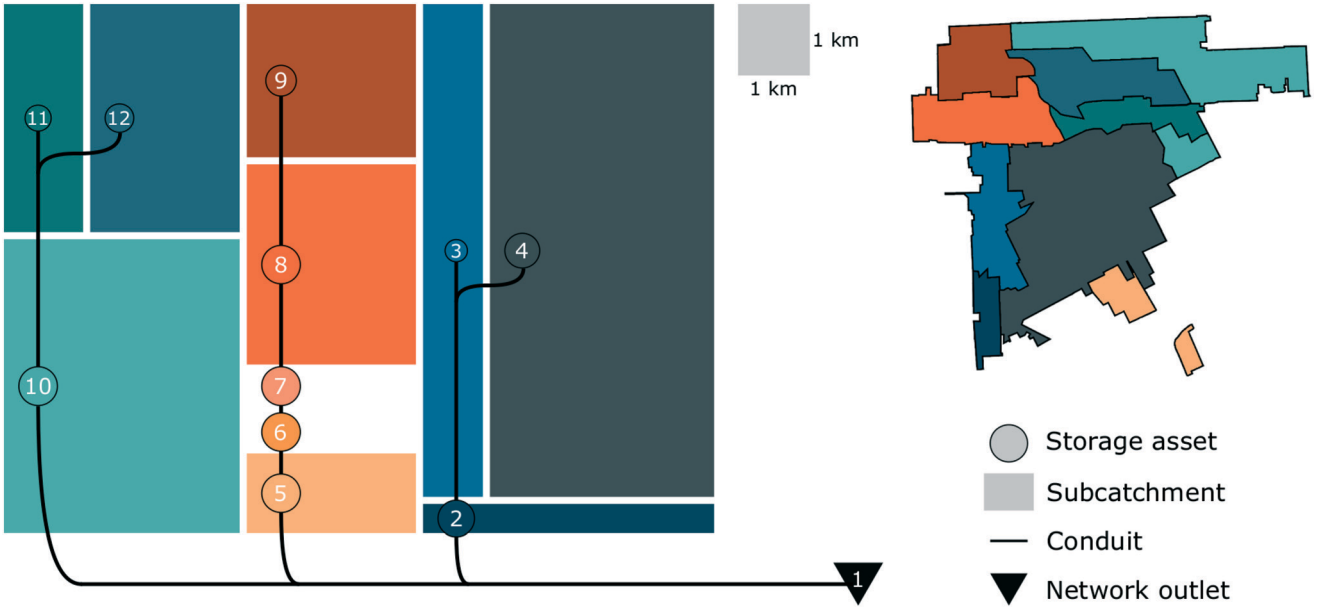

Fig. 2 System subcatchments and network topology of the case study collection system. Numbered, circular nodes in network topology represent upstream storage assets; relative size of circles indicate the diameter of the in-line conduit. Relative areas of the rectangles represent subcatchment areas that directly contribute to the corresponding storage asset. System physical dimensions are provided in Table S1.†

in each upstream storage asset would be required to ensure that recommended TSS loads are released. The gate position is then calculated from the desired flow at each upstream asset *via* orifice and weir equations.[48] More details for this implementation can be found in the public web repository (https://github.com/stroutm/LBCsewer).

2.2.2 System water quality model. In the SWMM model, TSS is modeled using built-in pollutant model structures.[49] The build-up of TSS on subcatchments follows a power structure:

$$B = \min\left(C_1, C_2 \cdot t^{C_3}\right),$$

where B is the pollutant build-up (mass per unit area), C_1 is the maximum possible build-up (mass per unit area) (16 kg ha^{-1}, 14.275 lbm ac^{-1}), C_2 is the build-up rate (mass per unit area per day) (7 kg ha^{-1} per day, 6.245 lbm ac^{-1} per day), t is the antecedent dry period length (t^{-C_3}), and C_3 is the exponent. The subcatchment wash-off function is exponential:

$$W = E_1 \cdot q^{E_2} \cdot B,$$

where W is the pollutant wash-off (mass per area per hour), E_1 is the wash-off coefficient (0.5 mm^{-1}, 12.7 in^{-1}), E_2 is the wash-off exponent (1.5), q is the runoff rate (in h^{-1}), and B is the pollutant remaining build-up (mass per area). TSS model structure and parameter values were taken from previous studies.[49,50] TSS removal at each upstream asset considered both settling, as a function of depth in the storage pipe, and resuspension, as a function of flow through the storage pipe:

$$R = 1 - \exp\left(-\frac{v_s \cdot \Delta t}{\mathrm{DEPTH}}\right) - \exp\left(-\frac{a \cdot b}{\mathrm{FLOW}}\right),$$

where R denotes the percent removal of TSS concentration, v_s is the settling velocity (determined by aggregating the solids classes in Gaborit *et al.*[50] to yield 0.00419 ft s^{-1}), Δt is the time step, DEPTH is the water depth in the storage pipe, a is a ratio between velocity and TSS resuspension to result in 100% resuspension for the maximum velocity through the storage pipe, b is a linear approximation of the ratio between flow and velocity computed for each upstream in-line storage asset, and FLOW is the flow through the storage pipe. The assumption of a single settling velocity for all particles is a simplification made here to narrow the focus of this study. Note that this is a simplification of the representation of the underlying physical system; it merely serves as a simulation choice. The control approach described above requires only measured states from the system, not an entire model. Thus, whether implemented on a more complex simulation model or on a real-world system with sensors, this control algorithm would remain the same in structure and implementation.

2.2.3 Performance evaluation. The performance of the control algorithm was evaluated across an entire year, using the precipitation time series in ESI† (Fig. S2). The dynamic behavior was evaluated by plotting the time series of controlled and uncontrolled scenarios. The aggregate performance was also summarized across the whole year, using a set of performance metrics while varying the control parameters (ρ, α_1^q, and α_1^{tss}). To reflect real world implementation, control decisions were constrained to a 15 minute window.

Specifically, six performance metrics are evaluated: WRRF flow and TSS load variance during dry-weather periods, comparison of controlled and uncontrolled WRRF flow and TSS load peaks, TSS mass remaining in the sewer network,

and flooding volume. Dry-weather periods are defined by the precipitation data as being a full 24 hours after the last occurrence of rain to simplify evaluation. During these periods, flow variance is computed by

$$\frac{1}{T}\sum_{t=1}^{T}\left(S_1^{\mathrm{q}}(t)-\overline{S}_1\right)^2,$$

where $S_1^{\mathrm{q}}(t)$ is the WRRF flow at time step t, $\overline{S}_1$ is the average WRRF flow over the dry-weather periods, and T is the total length of the dry-weather periods.[51] The WRRF TSS load variance is computed similarly. Note that these are computed with respect to absolute, not normalized, flow and TSS load values and so scale will be indicative of respective units. This dry-weather variance provides a measure of deviation from the mean dry-weather flow or TSS load, indicating how "flat" inflow dynamics are, that is a variance of zero indicates perfect steady-state inflow conditions during dry-weather periods, which is beneficial for steady-state operation at the WRRF. To focus on wet-weather peaks, peak height is defined to be the amount of flow or TSS load above the maximum dry-weather flow or TSS load, respectively. While this would ideally be evaluated on a storm-specific basis, to automate this calculation the peak reduction is averaged across each week of the simulation period. Peak reduction is then computed as a normalized factor

$$1 - \mathrm{peak}_{\mathrm{controlled}}/\mathrm{peak}_{\mathrm{uncontrolled}}.$$

The TSS mass remaining in the sewer network is computed as the difference between the cumulative TSS load received by the WRRF, normalized against the uncontrolled cumulative TSS load:

$$\text{TSS remaining} = \frac{\sum_{t=1}^{T}\text{TSS load}_{\text{uncontrolled}}(t) - \sum_{t=1}^{T}\text{TSS load}_{\text{controlled}}(t)}{\sum_{t=1}^{T}\text{TSS load}_{\text{uncontrolled}}(t)}.$$

The volume of flooding is calculated in the flow routing statistics by the simulation of the SWMM input file *via* PySWMM. This flooding volume is then expressed as a fraction of total volume that passes through the network.

3 Results and discussion

This section is split into two parts. First, a number of specific control scenarios are carried out to evaluate the dynamic performance of the algorithm under a set of objectives and constant control parameters. The Scenario analysis section is split into three scenarios, which compare parameterization of the algorithm to (1) attenuate flows, (2) attenuate TSS loads, and (3) jointly balance flows and TSS loads at the WRRF. Second, a parameterization analysis is carried out to determine how specific weight combinations of the control parameters affect the performance of the controlled system.

3.1 Scenario analysis

3.1.1 Scenario 1: flow attenuation. The control algorithm is first implemented with the sole objective of attenuating downstream flows, wherein the upstream storage assets are guided to hold water to reduce the peaks of dry- and wet-weather events. The normalized downstream flow setpoint $S_1^{\mathrm{q}*}$ is 2.5, which was found to correspond with the maximum dry-weather flow. As such, the control algorithm tries to keep flow as close as possible to a steady-state without exceeding the maximum dry-weather flow. In this scenario α_1^{q} = 10.0, meaning that the priority of the downstream flow objective is weighted as being 10 times more important than the desire to keep each upstream storage asset empty. For this scenario, α_1^{tss} = 0.0 since there is no explicit consideration of water quality load dynamics.

Since the assets are controlled, water levels in the upstream storage assets are higher than the uncontrolled case, both during dry- and wet-weather events (Fig. 3a). This scenario is able to considerably attenuate wet-weather flow peaks and equalize dry-weather oscillations when compared to the uncontrolled case (Fig. 3d). Furthermore, since flows are reduced, the TSS load exiting the combined sewer system is attenuated as well (Fig. 3g). During the first two months of the simulation period, the wet-weather flow peaks at the outlet of the combined sewer system are reduced by an average of 94.17%, while wet-weather TSS load peaks are reduced by an average of 104.47% (controlled/uncontrolled peaks of 0.0583 and −0.0447, respectively; Table 1a). The dry-weather flow and TSS load oscillations are reduced as well; this can be quantified by flow and TSS load variance during dry-weather days, which is reduced by 78.7% and 78.8%, respectively, from the uncontrolled case (Table 1a).

As expected, the control of storage assets reduces peak inflows at the WRRF (Fig. 3d). The control not only attenuates peak storm flows, but also reduces the variability of the diurnal flows (Table 1a). This is due to the utilization of upstream assets, which now strategically hold back water. Overall, the storage assets with relatively higher water levels during storms are generally those with higher contributing and upstream subcatchment areas (in particular, subcatchments 2, 4, 10). Since these assets are more stressed during storms, the control algorithm holds water in the remaining assets to balance storage capacity across the system. While this scenario does not explicitly control for TSS going to the WRRF, TSS loads are impacted positively because some TSS is held back in the upstream assets. As such, it can be expected that TSS peaks could be reduced even further by weighting TSS load, which is done in the next scenario.

3.1.2 Scenario 2: TSS load attenuation. Compared to the prior scenario, the second scenario parameterizes the control algorithm to focus solely on attenuating TSS load dynamics (α_1^{tss} = 10.0), without placing any weight on the flow dynamics (α_1^{q} = 0.0). The normalized downstream TSS load setpoint $S_1^{\mathrm{tss}*}$ is 2.5, to correspond with the maximum dry-weather TSS

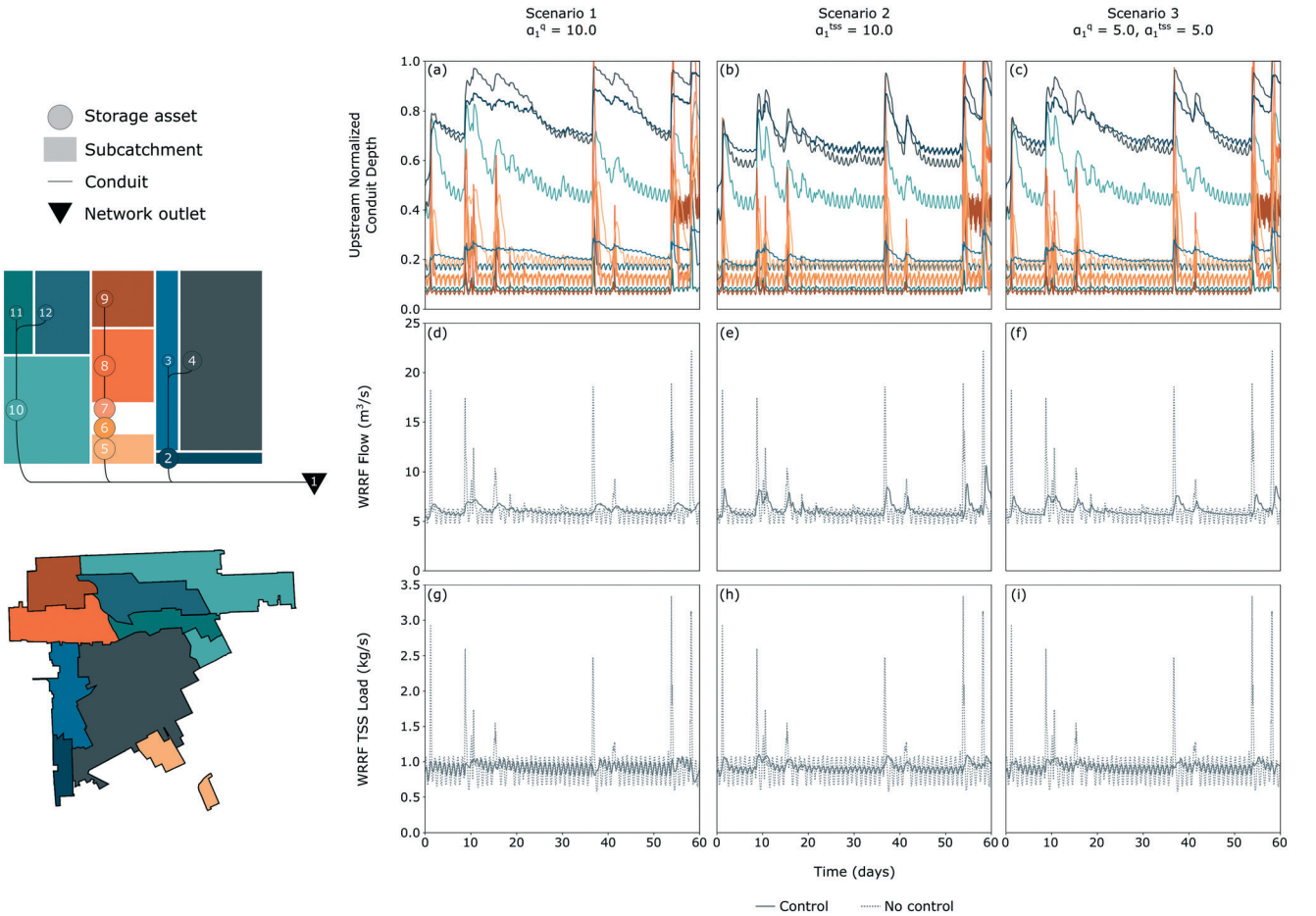

Fig. 3 Comparison of three control scenarios during the first two months of the simulation period. Scenario 1 places an emphasis on flow control, scenario 2 emphasizes TSS regulation, and scenario 3 balances both flow and water quality. The top row shows the upstream normalized depth behind the controlled storage assets in the network. The flow and TSS load at the network outlet are shown in the second and third rows. Dashed and solid lines in (d)–(i) denote uncontrolled and controlled cases, respectively. Subfigures (a)–(c) only show results from the controlled case for clarity.

Table 1 Summary of results in Fig. 3 for the first two months of the simulation period; a summary of results for the one year period is included in Fig. 4. Negative values for ratio of peak flows indicate that, on average, wet-weather peaks were reduced to below the maximum dry-weather levels. The scales of variances are indicative of their respective units

	Uncontrolled	(a) Flow control attenuation α_1^q = 10.0	(b) TSS control attenuation α_1^{tss} = 10.0	(c) Flow and TSS control attenuation α_1^q = 5.0, α_1^{tss} = 5.0
Ratio of peak flows (controlled/uncontrolled)	—	0.0583	0.2176	0.1320
Ratio of peak TSS loads (controlled/uncontrolled)	—	−0.0447	−0.0361	−0.0413
Dry-weather flow variance	364.7	77.7	48.0	44.2
Dry-weather TSS load variance	9.37×10^{-2}	1.99×10^{-2}	6.37×10^{-3}	1.20×10^{-2}

load. As would be expected, this formulation achieves similar TSS load attenuation relative to the formulation that focuses on flow only. Compared to the uncontrolled case, TSS load peaks that result from wet-weather events are reduced by an average of 103.61% over the first two months of the study period (controlled/uncontrolled peaks of −0.0361; Fig. 3h and Table 1b). Since water is held to regulate solids, flows are naturally attenuated as well, with average reductions of 78.24% (controlled/uncontrolled peaks of 0.2176; Fig. 3e and Table 1b). This is a lesser degree of flow attenuation compared to scenario 1 since, during wet-weather, TSS concentration is generally diluted by stormwater.

This scenario exhibits improved equalization of the dry-weather TSS load oscillations. During the first two months of the simulation period, there is a 93.2% reduction in TSS load variance, as well as an 86.8% reduction in flow variance, during dry-weather days (Fig. 3e and h and Table 1b). Thus, there is improved TSS performance compared to the first scenario.

While both scenarios perform better than the uncontrolled case, there is naturally a trade-off when comparing one to the other. Placing more emphasis on regulating TSS load peaks adversely impacts flow peaks, and *vice versa*. The equalization of TSS load is most notable during dry-weather, during which the control assets are used to buffer daily TSS load oscillations into the WRRF.

3.1.3 Scenario 3: balancing flow and TSS load. A natural extension of the prior two scenarios is to combine the flow and TSS attenuation objectives. This is accomplished by giving the two system importances equal values ($\alpha_1^q = \alpha_1^{tss} = 5.0$). In this formulation, wet-weather flow and TSS load peaks are attenuated with an average peak reduction of 86.80% and 104.13%, respectively, during the first two months of the simulation period (controlled/uncontrolled peaks of 0.1320 and −0.0413, respectively; Fig. 3f and i and Table 1c). Further, similar to the above two scenarios, dry-weather diurnal wastewater oscillations are reduced; there is a reduction of 87.9% and 87.2% in flow and TSS load variance during dry-weather days, respectively (Table 1c). Overall, the equal weighing of flow and TSS objectives provides a middle ground relative to the first two scenarios, and perhaps a realistic strategy for real-world implementation. These weights do not have to be equal values of α_1^q and α_1^{tss}, however; this is explored in the next section.

3.2 Parameterization analysis

3.2.1 Balancing flow against TSS loads. To assess trade-off sensitivity of weighing flow and TSS load objectives, reduction in wet-weather peaks and dry-weather variance are averaged over a one-year simulation time period across various combinations of α_1^q and α_1^{tss} values (Fig. 4a–d). These plots can be interpreted through the ratio of α_1^q and α_1^{tss}, which conveys how the relative magnitude of each parameter impacts system-wide performance. Furthermore, the absolute value of each parameter conveys how upstream assets are weighted against those downstream: as α_1^q and α_1^{tss} increase in magnitude, the downstream WRRF objectives are weighed more than those of upstream assets (Fig. 4a). In general, the trend for wet-weather peak reduction and dry-weather variance reduction for both flow and TSS load at the sewer network outlet is similar: larger system importance values result in better downstream performance by way of greater peak reduction and damped dry-weather oscillations. This is due to increased priority on maintaining the downstream flow and/or TSS load below the given thresholds as compared to the upstream objective of emptying storage assets. This implies that, when only considering downstream objectives, control with larger system importance values α_1^q and α_1^{tss} will result in smoother, more constant sewer network outflow and TSS load during both dry- and wet-weather periods compared to an uncontrolled case.

The flow system importance value α_1^q has more influence on both flow and TSS load peak reduction than the TSS load system importance value α_1^{tss} (Fig. 4a and b). Further, the TSS load system importance α_1^{tss} has more impact than the flow system importance α_1^q on dampening the dry-weather TSS load oscillations (Fig. 4d).

While the coordinated control of upstream sewer storage assets can be used to achieve flow and water quality objectives at the network outlet, this control must be sensitive to its impacts on other sewer dynamics that are important for the conveyance of water and pollutants through the network. First, the reduction of wet-weather flow and TSS load peaks at the combined sewer outlet can result in over-utilization of in-line storage assets, meaning that storage assets in the sewer will become fuller as capacity is allocated to the downstream outlet, and ultimately increase risk of network flooding. This is particularly pronounced during wet-weather events, as large volumes of water rapidly enter the sewer system as the contributing subcatchments drain. Thus, maintaining strict feedback control over storage assets can result in unanticipated flooding if upstream assets are used too liberally to hold water. Examples of this can be seen in Fig. 3a–c during wet-weather events. Fig. 4e demonstrates how system importance values, α_1^q and α_1^{tss}, impact this over-utilization and the volume of network flooding by the control algorithm. Both simulation and intuition confirm that lower system importance values for downstream objectives result in a reduction in flooding volume; this is particularly true for the flow system importance α_1^q. As discussed above, due to the settling and resuspension of TSS within the storage assets and the dilution of TSS during wet-weather events, less upstream storage capacity is required to attenuate TSS load peaks when compared to flow peaks during wet-weather events. As a result, even the moderately high values of α_1^{tss} considered here result in minimal flooding volume when compared to α_1^q values of a similar magnitude.

A second effect of control on the system is the accumulation of solids in the sewer system. Combined sewer flows have a relatively high concentration of solids resulting from the wastewater flows; typical untreated municipal wastewater has a TSS concentration range of 100–400 mg L^{-1}.[1] As a result, the settling of solids occurs due to increased and long-duration storage of combined sewer flows behind sewer assets. In order to minimize the magnitude of flow and/or TSS load peaks, stored flows must be slowly released, resulting in low velocities from the storage assets and minimal resuspension of settled solids in the sewer network. This allows for settled solids to accumulate in the sewer network. However, most sewers are not designed to manage these solids in the conveyance network and must employ significant maintenance efforts to manually remove these solids or flush them downstream.[2] Hence, control algorithms that operate or inform combined sewer control actions should be designed with solids accumulation as a key consideration. The impact of system importance parameters, α_1^q and α_1^{tss}, on solids accumulation is shown in Fig. 4f.

When TSS load is more strongly weighted than flow (*i.e.*, below the 1 : 1 line), the sewer network retains less solids mass within the storage assets; this is because flows are released based on the stored TSS concentrations in order to maintain a TSS load threshold downstream. At storage assets experiencing greater settling, the suspended solids

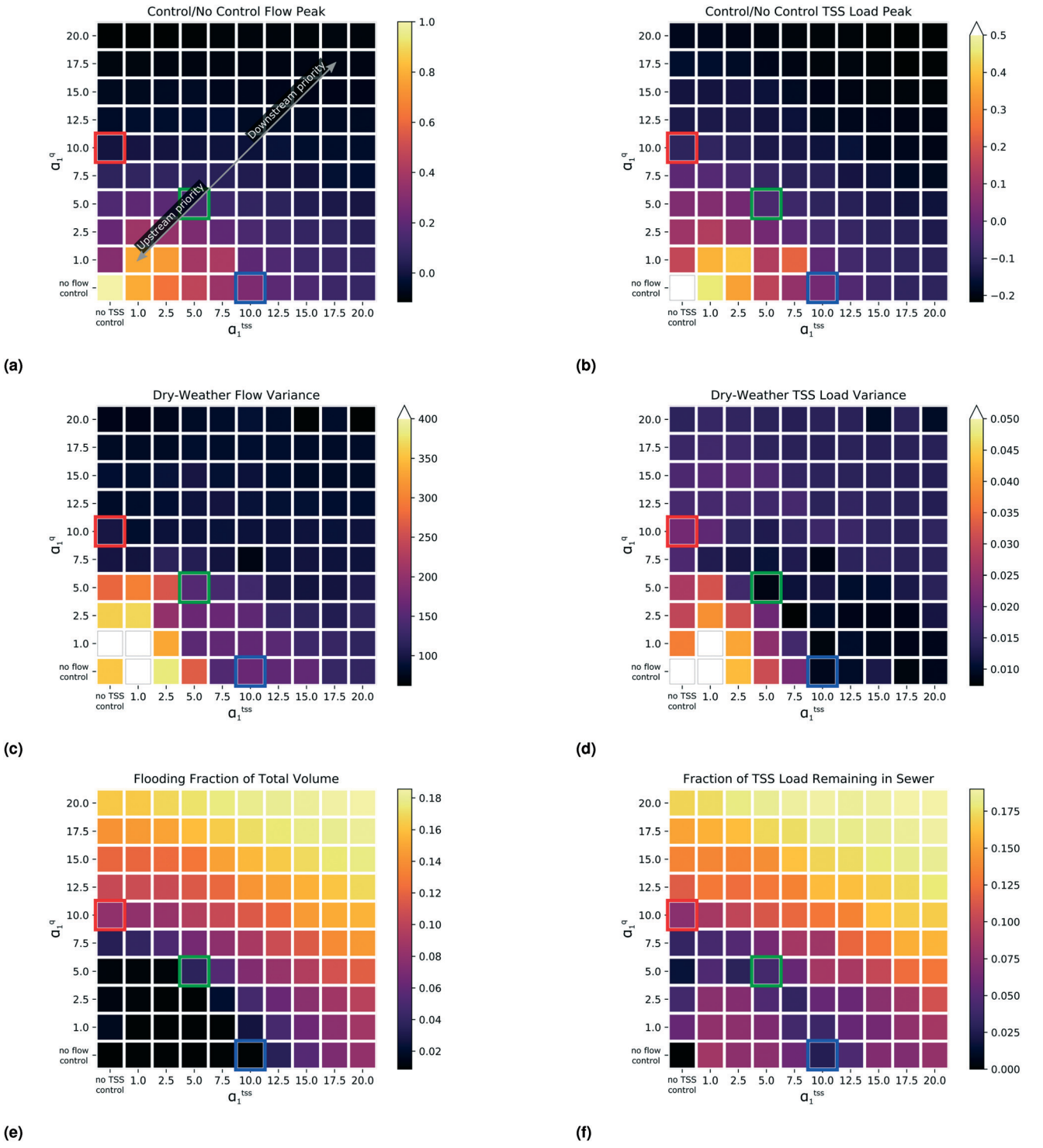

Fig. 4 Impact of system importance values on performance metrics, including (a) ratio of flow peak, (b) ratio of TSS load peak, (c) dry-weather flow variance, (d) dry-weather TSS load variance, (e) fraction of total volume that floods within the sewer, and (f) fraction of TSS load remaining in the sewer. Red, blue, and green boxes indicate selected parameter scenarios highlighted in Fig. 3 for scenarios 1, 2, 3, respectively. In all figures, a darker color indicates better performance in that particular metric. In (a) and (b), negative values for ratio of peak flows indicate that, on average, wet-weather peaks were reduced to below the maximum dry-weather levels.

concentration will be lower, thus requiring larger volumes to be released, resulting in resuspension. On the other hand, high flow system importance values ($\alpha_1^q \geq 12.5$) consistently resulted in greater than 10% solids retention within the upstream assets, regardless of the TSS load weight. This is likely due to the requirement for flows to be gradually released from the upstream storage assets to achieve flow attenuation and equalization at the downstream network

outlet. However, in achieving this, flows are released slowly, resulting in little solids resuspension and thus solids accumulation in the upstream storage assets.

3.2.2 Willingness to hold water. The formulation of the control algorithm presented here also includes the instantaneous importance weight ρ, which determines the willingness of an asset to hold water as levels approach storage capacity. For flow and TSS peak reduction, and dry-weather flow and TSS load variance, a lower ρ value is associated with better performance (Fig. 5, where $\alpha_1^q = \alpha_1^{tss} = 5.0$). However, for most of these first four metrics, the range of performance does not vary greatly with the values of ρ considered here, compared with the range of performance values in Fig. 4. The exception to this is dry-weather flow variance. In this case, lower ρ values perform considerably better than higher ρ values (Fig. 5 and S3†). This is because storage assets fill up with diurnal inflows, and suddenly release flows when at capacity. Lower ρ values buffer this variability by more steadily releasing water and reducing impulses to the WRRF.

The impact of the instantaneous importance weight ρ is also assessed for network flooding and solids accumulation (Fig. 5). While all ρ values considered here produce little flooding, flooding volume is inversely proportional to ρ value. To account for this behavior with respect to flooding, note that upstream storage assets with higher normalized depths, and thus higher risk for flooding, will release more water than those that are not prone to overflowing at that particular time. Further, ρ has little impact on the solids load remaining in the sewer network, though there is minimal improvement in resuspension with higher ρ values (Fig. 5).

3.3 Towards implementation

A natural extension from these findings would be the separation and customization of control schemes for various system states and inputs. The results suggest a benefit in adjusting control regimes or parameterizations between wet- and dry-weather periods (Fig. 3 and Table 1). Flow attenuation (scenario 1) resulted in higher flow peak reduction during wet-weather when compared to TSS load attenuation (scenario 2) (94.17% *vs.* 78.24%, respectively); however, dry-weather flow and TSS load oscillations were not dampened as successfully *via* flow attenuation (scenario 1) as with TSS load attenuation (scenario 2) (flow oscillation damped: 78.7% *vs.* 86.8% and TSS load oscillation damped: 78.8% *vs.* 93.2%). Thus, in this case, flow-driven control during wet-weather events and TSS load-driven control during dry-weather periods would be a viable strategy towards improving sewer operation. Indeed, having weather-dependent regimes is a common strategy in more manual sewer operations.[35,37,52] As such, implementations should also look beyond one-size-fits-all parameterizations in the case of real-time control.

Further, while the system importance parameter assignment has been demonstrated to achieve improved downstream performance (*e.g.*, peak reduction and oscillation dampening), beyond a certain level of weighting, downstream performance plateaus (α_1^q, $\alpha_1^{tss} \geq 10$, Fig. 4a–d). What should determine system importance parameter values is a balance with upstream or system-wide performance indicators (*e.g.*, flooding, solids accumulation). In this study, there is an upper limit on downstream system importance values to minimize network flooding (α_1^q, $\alpha_1^{tss} \leq 10$; Fig. 4e). One approach to mitigate network flooding would be to build in a heuristic rule for releasing stored water when an asset becomes too full. However, maintaining a connection with actual implementation, this strategy would need to ensure that the emergency release of stored water from upstream assets does not result in too great a surge of flows at downstream storage assets or the WRRF inlet.

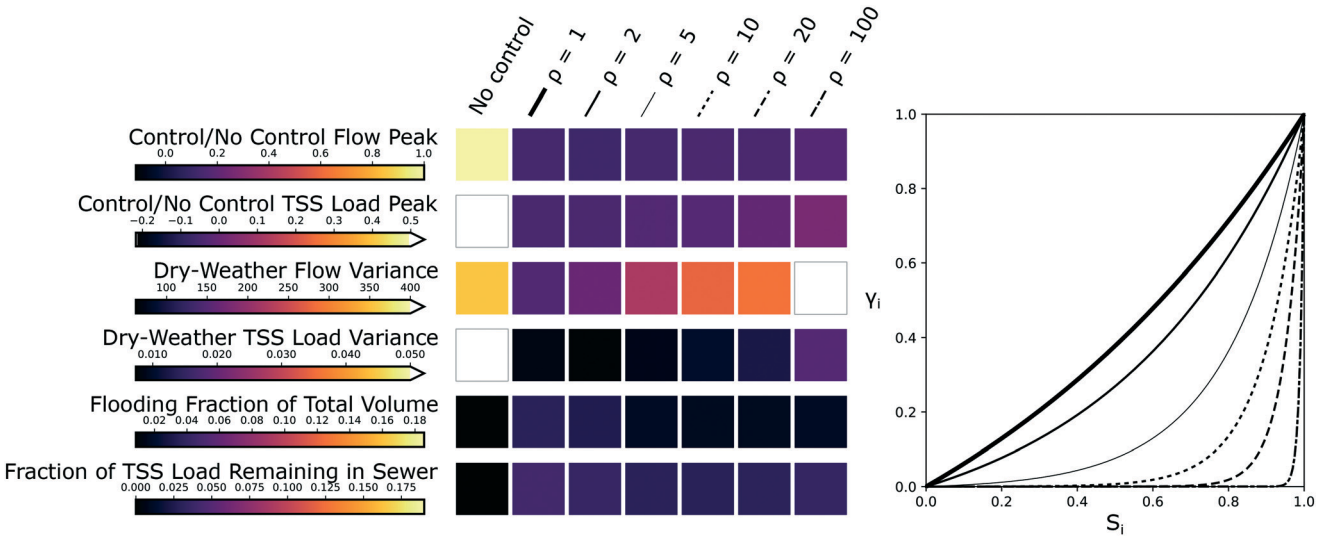

Fig. 5 Impact of instantaneous importance weight ρ on performance metrics for $\alpha_1^q = \alpha_1^{tss} = 5.0$. The right graph demonstrates the relationship between state S_i and instantaneous importance γ_i for each ρ value for reference. In all scales, a darker color indicates better performance in that particular metric.

More interestingly, perhaps, is the presence of a band of higher performance for solids accumulation across system importance values (for system importance values such that $\alpha_1^q + \alpha_1^{tss} \approx 10$; Fig. 4f). To explain this, note that settling and resuspension are dictated by water depth and velocity of releases. For lower system importance values, there is shallow upstream storage and thus less distance for solids to settle, and hence more settling. However, the shallow storage also results in lower velocity when water is released, and thus less resuspension. On the other hand, high system importance values result in large quantities of water stored behind upstream assets, requiring small releases due to the strict control against downstream peaks — and thus minimal resuspension of settled solids. However, between these ranges is an area of minimal solids accumulation. This indicates not only a trade-off between high and low system importance values with down- and upstream performance, but a desirable range of values for the control algorithm parameters. In this case study, the most desirable performance across all considered system-wide metrics would be achieved with system importance values that satisfy $\alpha_1^q + \alpha_1^{tss} \approx 10$ and $\rho = 1$ (Fig. 4 and 5). These parameters may be case study-specific, and parameter values for other systems may likely vary based on context and system priorities; this will be explored in future work so that transferability of results can be considered. More generally, this illustrates the need for optimization and parameter analysis in formulating the control problem and determining priority weights in the objective function. Similar conclusions can also be found in other studies that highlight the impact of parameterization on control performance and stability.[53,54] Overall, this lends support to trying out a simpler control technique first — such as the one presented in this paper — before embarking on the application of more complex algorithms. A first order, simpler analysis may shed insights on performance bands unique to a given system, which may provide insight to tuning more complex algorithms.

Complex and interesting dynamics may be missed if control algorithm formulations fail to account for a breadth of upstream and downstream performance measures. Namely, optimization of one parameter may often come at the cost of another. Indeed, the concern of sewer solids accumulation has been explored in other works.[13] While control algorithms for water systems are typically formulated, tested, and refined in simulation, connection and communication with real-world system operators is crucial to the feasibility of real-time control implementation. For instance, attempting to maintain downstream flow and/or TSS load strictly below a threshold may be too restrictive given available storage in sewer assets during high-stress times (*e.g.*, large and/or flashy storms) and would thus require over-utilization of storage assets insomuch as they exceed their storage capacity and increase the risk of flooding in the network and may increase in-line maintenance needs. This study explored this balance between upstream and downstream objectives using parameters within the control algorithm, namely system importance values α_1^q and α_1^{tss} and instantaneous importance weight ρ. The realizable values of these parameters will ultimately not be governed solely by physical constraints, but also human preferences.

The results illustrated here demonstrate a need for further flexibility to avoid or manage the accumulation of settled solids behind control assets in the sewer network. Extending beyond the approach discussed here, this flexibility can be incorporated by introducing dewatering strategies or intentional scour release events that occur after wet-weather events by releasing water from upstream to downstream assets, thereby flushing the system to encourage resuspension and conveyance of solids to the downstream WRRF for treatment and management.[2,55]

4 Conclusion

In this study, we demonstrate the use of a control algorithm, flexible to multiple water quantity and quality objectives, as well as downstream and upstream objectives. Our parameterization analysis is used to explore trade-offs among these goals. Our findings highlight the importance of identifying a range of near-optimal parameter values for control algorithms. Future work should investigate how these regions translate to other algorithm formulations. It is critical to note that what defines "optimal" will be dependent on the system context, human preferences, and trade-offs between multiple objectives. Overall, bands of near-optimality may arise and string a balance between most objectives. This however, should be evaluated on a case-by-case basis. In lieu of one optimal point, this may present a range of aspirational values to appeal to system operators. Sensitivity analyses and decision maker preferences should be considered in the control process as early as the formulation of the actual control problem and objective function.

Conflicts of interest

There are no conflicts to declare.

Acknowledgements

This material is based upon work supported by the National Science Foundation Graduate Research Fellowship Program under Grant No. DGE 1256260, as well as the National Science Foundation Smart and Connected Communities Program under Grant No. 1737432. Any opinions, findings, and conclusions or recommendations expressed in this material are those of the authors and do not necessarily reflect the views of the National Science Foundation.

References

1 Metcalf & Eddy, Inc., G. Tchobanoglous, F. L. Burton and H. D. Stensel, *Wastewater Engineering: Treatment and Resource Recovery*, McGraw-Hill, 5th edn, 2013.
2 U.S. Environmental Protection Agency, Flow Equalization, 1974.

3 S.-Y. Leu, D. Rosso, L. E. Larson and M. K. Stenstrom, *Water Environ. Res.*, 2009, **81**, 2471–2481.
4 R. C. Leitão, A. C. Van Haandel, G. Zeeman and G. Lettinga, *Bioresour. Technol.*, 2006, **97**, 1105–1118.
5 C. P. L. Grady, Jr., G. T. Daigger, N. G. Love and C. D. M. Filipe, *Biological Wastewater Treatment*, CRC Press, 2011.
6 J. Bolmstedt, *PhD thesis*, Lund University, 2004.
7 I. Aymerich, L. Rieger, R. Sobhani, D. Rosso and L. Corominas, *Water Res.*, 2015, **81**, 113–123.
8 M. Gatterdam and R. Johnson, *Proceedings of the Water Environment Federation*, 2016, pp. 1853–1868.
9 P. van Daal, G. Gruber, J. G. Langeveld, D. Muschalla and F. Clemens, *Environ. Model. Softw.*, 2017, **95**, 90–101.
10 N. S. V. Lund, A. K. V. Falk, M. Borup, H. Madsen and P. S. Mikkelsen, *Crit. Rev. Environ. Sci. Technol.*, 2018, **48**, 279–339.
11 M. Schütze, A. Campisano, H. Colas, W. Schilling and P. A. Vanrolleghem, *J. Hydrol.*, 2004, **299**, 335–348.
12 H. Colas, M. Pleau, J. Lamarre, G. Pelletier and P. Lavallee, *Water Qual. Res. J. Can.*, 2004, **39**, 466–478.
13 R. M. Ashley, J. Dudley, J. Vollertsen, A. J. Saul, A. Jack and J. R. Blanksby, *Water Sci. Technol.*, 2002, **45**, 239–246.
14 A. Campisano, J. Cabot Ple, D. Muschalla, M. Pleau and P. A. Vanrolleghem, *Urban Water J.*, 2013, **10**, 300–311.
15 B. Kerkez, C. Gruden, M. Lewis, L. Montestruque, M. Quigley, B. Wong, A. Bedig, R. Kertesz, T. Braun, O. Cadwalader, A. Poresky and C. Pak, *Environ. Sci. Technol.*, 2016, **50**, 7267–7273.
16 G. Weinrich, W. Schilling, A. Birkely and T. Moland, *Water Sci. Technol.*, 1997, **36**, 331–336.
17 W. Schilling, B. Andersson, U. Nyberg, H. Aspegren, W. Rauch and P. Harremoës, *Journal of Hydraulic Research*, 1996, **34**, 785–797.
18 L. García, J. Barreiro-Gomez, E. Escobar, D. Téllez, N. Quijano and C. Ocampo-Martinez, *Adv. Water Resour.*, 2015, **85**, 120–132.
19 M. Jørgensen, W. Schilling and P. Harremoës, *Water Sci. Technol.*, 1995, **32**, 249–257.
20 G. Cembrano, J. Quevedo, M. Salamero, V. Puig, J. Figueras and J. Mart, *Control Engineering Practice*, 2004, **12**, 1–9.
21 C. Ocampo-Martinez, *Model predictive control of wastewater systems*, Springer, 2010, pp. 1–236.
22 C. Sun, B. Josep-Duran, G. Cembrano, V. Puig and J. Meseguer, *EPiC Series in Engineering: International Conference on Hydroinformatics*, 2018, pp. 2033–2041.
23 K.-J. van Heeringen, J. Gooijer and D. Schwanenberg, *EGU General Assembly Conference Abstracts*, 2013.
24 L. A. Montestruque, *Smart Water Grids: A Cyber-Physical Systems Approach*, CRC Press, 2018, ch. 6, pp. 151–168.
25 M. Bartos, B. Wong and B. Kerkez, *Environ. Sci.: Water Res. Technol.*, 2018, **4**, 346–358.
26 A. Mullapudi, B. P. Wong and B. Kerkez, *Environ. Sci.: Water Res. Technol.*, 2017, **3**, 66–77.
27 E. Gaborit, F. Anctil, G. Pelletier and P. Vanrolleghem, *Urban Water J.*, 2016, **13**, 841–851.
28 D. Muschalla, B. Vallet, F. Anctil, P. Lessard, G. Pelletier and P. A. Vanrolleghem, *J. Hydrol.*, 2014, **511**, 82–91.
29 S. Sharior, W. McDonald and A. J. Parolari, *J. Hydrol.*, 2019, **573**, 422–431.
30 J. F. Carpenter, B. Vallet, G. Pelletier, P. Lessard and P. A. Vanrolleghem, *Water Qual. Res. J. Can.*, 2014, **49**, 124–135.
31 A. Gilpin and M. Barrett, *World Environmental and Water Resources Congress*, 2014, pp. 65–74.
32 S. Eggimann, L. Mutzner, O. Wani, M. Y. Schneider, D. Spuhler, M. Moy de Vitry, P. Beutler and M. Maurer, *Environ. Sci. Technol.*, 2017, **51**, 2538–2553.
33 M. Mahmoodian, O. Delmont and G. Schutz, *International Journal of Sustainable Development and Planning*, 2017, **12**, 98–111.
34 E. Meneses, M. Gaussens, C. Jakobsen, P. Mikkelsen, M. Grum and L. Vezzaro, *Water*, 2018, **10**, 76.
35 A. L. Mollerup, P. S. Mikkelsen, D. Thornberg and G. Sin, *Urban Water J.*, 2017, **14**, 435–442.
36 M. Pleau, H. Colas, P. Lavallée, G. Pelletier and R. Bonin, *Environ. Model. Softw.*, 2005, **20**, 401–413.
37 D. Fiorelli, G. Schutz, K. Klepiszewski, M. Regneri and S. Seiffert, *Urban Water J.*, 2013, **10**, 342–353.
38 P. Borsányi, L. Benedetti, G. Dirckx, W. De Keyser, D. Muschalla, A.-M. Solvi, V. Vandenberghe, M. Weyand and P. A. Vanrolleghem, *J. Environ. Eng. Sci.*, 2008, **7**, 395–410.
39 A. Campisano, W. Schilling and C. Modica, *Urban Water*, 2000, **2**, 235–242.
40 G. Dirckx, M. SchÃitze, S. Kroll, C. Thoeye, G. De Gueldre and B. Van De Steene, *Urban Water J.*, 2011, **8**, 367–377.
41 L. Vezzaro and M. Grum, *J. Hydrol.*, 2014, **515**, 292–303.
42 S. Kroll, G. Dirckx, B. M. Donckels, M. Van Dorpe, M. Weemaes and P. Willems, *Water Sci. Technol.*, 2016, **73**, 1637–1643.
43 M. Marinaki and M. Papageorgiou, *European Control Conference*, 2003, pp. 2407–2412.
44 S. Darsono and J. W. Labadie, *Environ. Model. Softw.*, 2007, **22**, 1349–1361.
45 B. P. Wong and B. Kerkez, *Water Resour. Res.*, 2018, **54**, 7309–7330.
46 S. P. Rimer, A. Mullapudi, S. C. Troutman and B. Kerkez, *Proceedings of the 10th ACM/IEEE International Conference on Cyber-Physical Systems - ICCPS '19*, 2019, pp. 350–351.
47 Open Water Analytics, PYSWMM, https://github.com/OpenWaterAnalytics/pyswmm, 2019.
48 L. A. Rossman, *Storm Water Management Model User's Manual Version 5.1*, 2015.
49 L. A. Rossman and W. C. Huber, *Storm Water Management Model Reference Manual Volume III - Water Quality*, 2015.
50 E. Gaborit, D. Muschalla, B. Vallet, P. A. Vanrolleghem and F. Anctil, *Urban Water J.*, 2013, **10**, 230–246.
51 M. Bartos and B. Kerkez, *Adv. Water Resour.*, 2019, **127**, 167–179.
52 A. L. Mollerup, P. S. Mikkelsen, D. Thornberg and G. Sin, *Environ. Model. Softw.*, 2015, **66**, 153–166.
53 S. Kroll, M. Weemaes, J. Van Impe and P. Willems, *Water*, 2018, **10**, 1675.
54 A. L. Mollerup, P. S. Mikkelsen and G. Sin, *Environ. Model. Softw.*, 2016, **83**, 103–115.
55 Z. Yuan, G. Olsson, R. Cardell-Oliver, K. van Schagen, A. Marchi, A. Deletic, C. Urich, W. Rauch, Y. Liu and G. Jiang, *Water Res.*, 2019, **155**, 381–402.